

# High-Temperature Polymerization of Styrene: Mechanism Determination with Preparative Gel Permeation Chromatography, Matrix-Assisted Laser Desorption/Ionization Time-of-Flight Mass Spectrometry, and $^{13}\text{C}$ Nuclear Magnetic Resonance

J. D. Campbell,<sup>1</sup> J. A. Allaway,<sup>1</sup> F. Teymour,<sup>2</sup> M. Morbidelli<sup>3</sup>

<sup>1</sup>Johnson Polymer, 8310 16<sup>th</sup> Street, Sturtevant, Wisconsin 53177-0902

<sup>2</sup>Department of Chemical Engineering, Illinois Institute of Technology, Chicago, Illinois 60616

<sup>3</sup>Swiss Federal Institute of Technology Zurich, Institut für Chemie- und Bioingenieurwissenschaften, ETH-Hönggerberg, CH-8093 Zurich, Switzerland

Received 9 February 2004; accepted 28 April 2004

DOI 10.1002/app.20914

Published online in Wiley InterScience (www.interscience.wiley.com).

**ABSTRACT:** An experimental study designed to elucidate mechanistic details regarding the thermal polymerization of styrene between 260 and 340°C is reported. The data show that back-biting to the third or fifth carbon from the chain end, followed by  $\beta$  scission, is the dominant chain-producing reaction in the molecular weight development. This conclusion is supported by the  $^{13}\text{C}$ -NMR data coupled with preparative gel permeation chromatography, which show that the predominant low-molecular-weight oligomers are 2,4-diphenyl-1-butene and 2,4,6-triphenyl-1-hexene, that is, the products of the 1:3 and 1:5 back-biting/ $\beta$ -scission reactions, respectively. The presence of head-to-head or head-to-tail branching, due to chain transfer to the polymer or

back-biting, is shown to be negligible through  $^{13}\text{C}$ -NMR analysis. Finally, the distribution of terminal unsaturations, determined by the relative rates of termination, back-biting, and chain transfer to polymer, has been measured with matrix-assisted laser desorption/ionization time-of-flight mass spectrometry. This has shown that the back-biting/ $\beta$ -scission reaction dominates the molecular weight development in comparison with either termination or chain transfer to the polymer. © 2004 Wiley Periodicals, Inc. *J Appl Polym Sci* 94: 890–908, 2004

**Key words:** NMR; MALDI; addition polymerization

## INTRODUCTION

The polymerization mechanism of styrene between 250 and 350°C involves a combination of thermal initiation through styrene activation, propagation, termination, and polymer degradation reactions. Each of these processes consists of a set of elementary reactions, strongly interacting with one another. When considered individually, these processes are relatively well understood.

The fact that styrene could undergo spontaneous free-radical polymerization was recognized very early on. However, it was Mayo<sup>1</sup> that first proposed the mechanism for the thermal initiation process. Subsequent work by Brown et al.,<sup>2</sup> Buchholz and Kirchner,<sup>3</sup> Kauffmann et al.,<sup>4</sup> Olaj et al.,<sup>5</sup> and Kirchner and Riederle<sup>6</sup>, refined the mechanism proposed by Mayo<sup>1</sup> into

the form currently widely accepted and shown in Figure 1.

The polymerization process consisted of the usual propagation, bimolecular termination, and chain-transfer reactions, the latter being more important than usual because of the increased hydrogen mobility at the higher temperatures considered. The degradation of polystyrene has been investigated extensively in the literature in the absence of polymerization by the continuous removal of the monomer *in vacuo*. The works of Jellinek,<sup>7,8</sup> Madorski,<sup>9</sup> Cameron and MacCallum,<sup>10</sup> Schroder et al.,<sup>11</sup> and Ebert et al.<sup>12</sup> present a fairly consistent picture of the underlying mechanism. At temperatures above 250°C, the process begins with a random hydrogen abstraction from a chain, followed by  $\beta$  scission in either the i or ii  $\beta$  position, as shown in Figure 2(a). Once the  $\beta$ -scission reaction occurs, producing a radical at the chain end, a variety of events can take place. It can undergo chain-end  $\beta$  scission [Fig. 2(b)], in which the carbon-carbon bond in the  $\beta$  position to the chain-end radical cleaves; this results in depropagation or unzipping. Alternatively, this radical can undergo back-biting to the third, fifth,

Correspondence to: M. Morbidelli (morbidelli@tech.chem.ethz.ch)

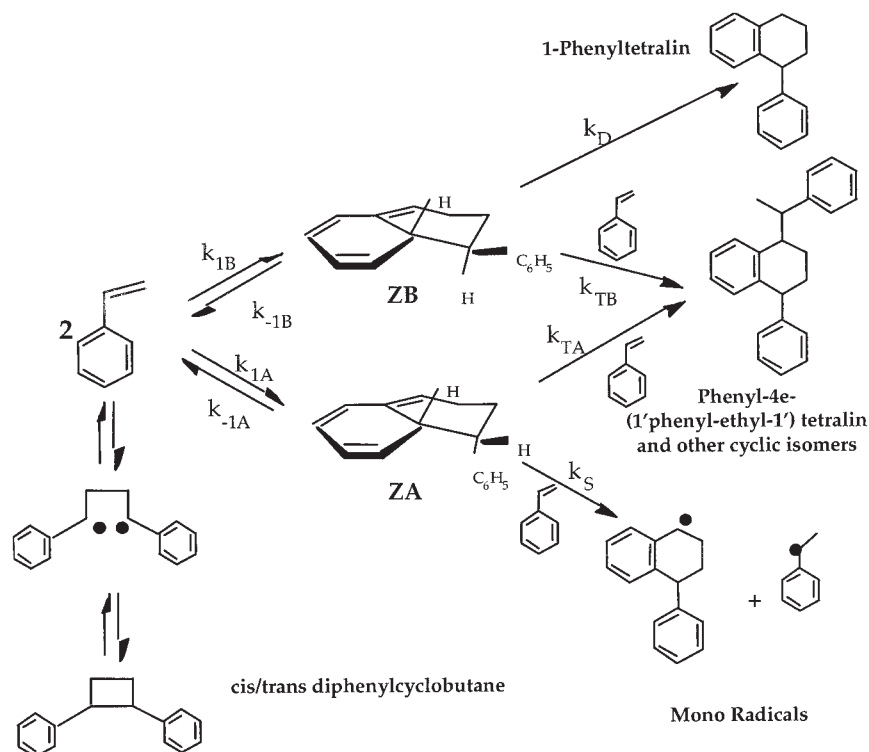


Figure 1 Thermal initiation mechanism for styrene.

or seventh carbon position [also shown in Fig. 2(b)]. Back-biting to the fifth carbon from the chain end is favored over the others because of the formation of the thermodynamically favored six-membered ring. The second, fourth, and sixth positions are not favored because of the difficulty of abstracting the secondary methylene hydrogens. Woo and Broadbelt<sup>13</sup> estimated that the dissociation energy of the secondary methylene hydrogen is approximately twice that of the tertiary benzylic hydrogen. This midchain radical can then undergo  $\beta$  scission in one of the two  $\beta$  positions, producing two smaller fragments, one radical and one polymer chain with a terminal double bond. It is generally assumed that there is an equal probability of breaking in either of the two possible  $\beta$  positions [i and ii in Fig. 2(a,b)]. This back-biting/ $\beta$ -scission mechanism has been proposed by many authors<sup>9-11,14-17</sup> and is widely accepted as the mechanism for the formation of the specific oligomers that are found in significant amounts in the products of polystyrene degradation. For example, the 1:5 back-biting reaction produces the oligomer 2,4,6-triphenyl-1-hexene (TPH), whereas 1:3 back-biting leads to 2,4-diphenyl-1-butene (DPB). Schroder et al.<sup>11</sup> studied the degradation of polystyrene at temperatures greater than 290°C and identified 13 low-molecular-weight byproducts, many of which were thermal initiation byproducts. However, the concentrations of DPB and TPH were among the highest, thus indicating the importance of

the back-biting reaction in the degradation process. On the other hand, Ohtani et al.<sup>17</sup> suggested that the 1:3 back-biting reaction is not the main route to the formation of DPB because of the high bond strain of the transition state, and they proposed a two-stage reaction in which a benzyl radical undergoes an addition-fragmentation reaction with a terminal double bond.

The question of whether polymer degradation is mainly dominated by back-biting followed by  $\beta$  scission (characteristic scission) or by random hydrogen abstraction followed by  $\beta$  scission [chain transfer to polymer (CTP)] has been debated for years in the literature, as discussed in the review by Cameron and MacCallum.<sup>10</sup> The reported experimental data seem to indicate that at high molecular weights random abstraction dominates, whereas at low molecular weights characteristic scission dominates. This is consistent not only with the previous observation that the oligomers are produced by characteristic scission but also with the fact that at a high melt viscosity, chain-end mobility is reduced, limiting back-biting and thus characteristic scission. McNeil et al.,<sup>16</sup> Ohtani et al.,<sup>17</sup> and Ide et al.<sup>18</sup> in fact concluded that at a low melt viscosity (the conditions of this study), characteristic scission is the dominant mechanism of degradation.

In addition to the  $\beta$ -scission degradation reaction, it is possible that a chain undergoes spontaneous thermal scission, by which a carbon-carbon bond in the

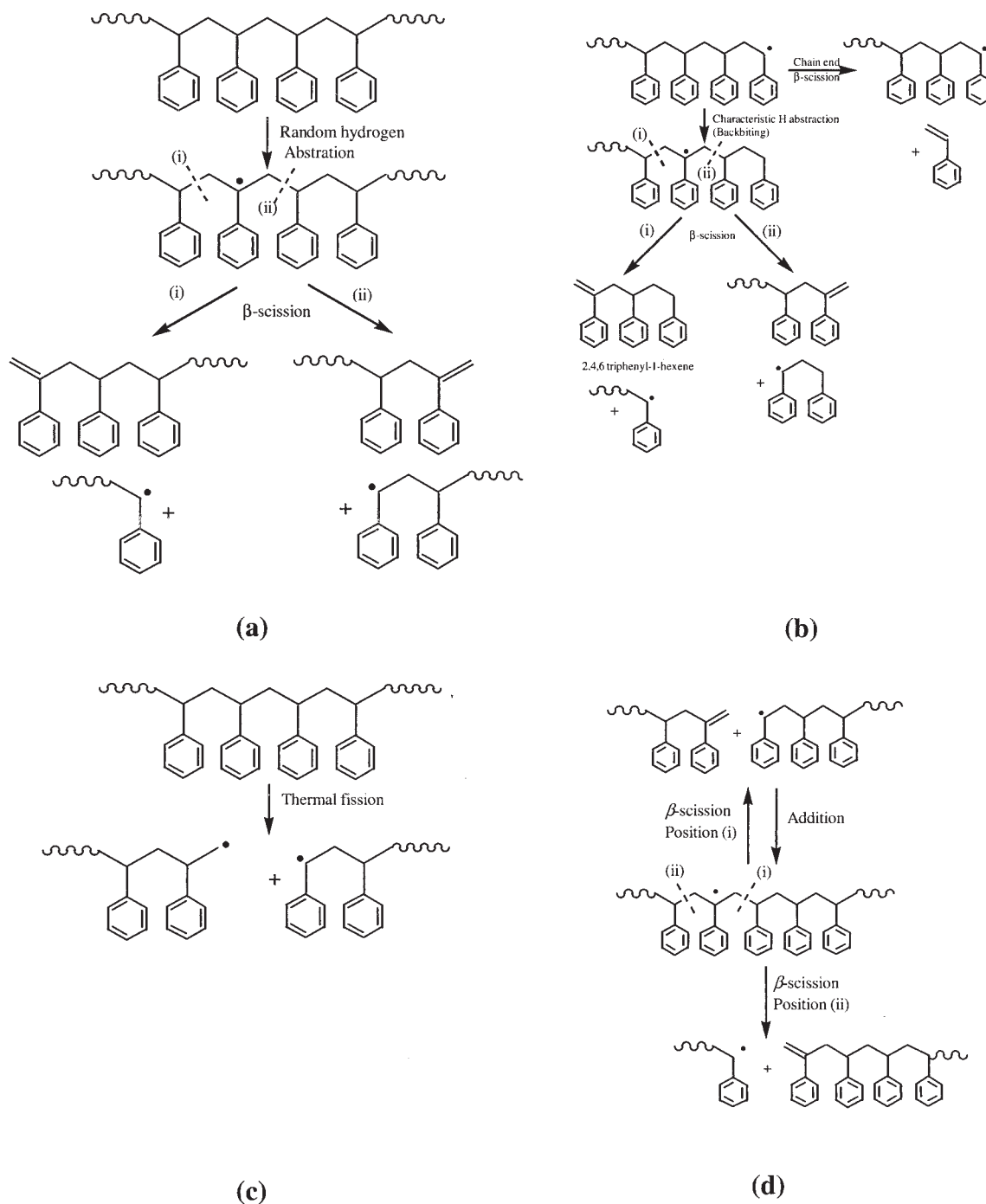


**Figure 2** Degradation mechanism of polystyrene: (a) the production of a midchain radical through random hydrogen abstraction, followed by  $\beta$  scission in one of the two possible  $\beta$  positions; (b) characteristic hydrogen abstraction, or back-biting, followed by  $\beta$  scission or chain-end  $\beta$  scission (depropagation); (c) thermal fission; and (d) addition–fragmentation.

polymer chain can break, forming two smaller radical fragments, as shown in Figure 2(c). This reaction has a high activation energy<sup>19</sup> and would be expected to be significant only at extreme temperatures.

The addition reaction between a growing polymer radical and a terminal unsaturation on a dead polymer chain produces a midchain radical that can also un-

dergo  $\beta$  scission. This addition–fragmentation reaction was first reported by Fisher and Luders<sup>20</sup> in polystyrene polymerization with 2,4-diphenyl-4-methyl-1-pentene [ $\alpha$ -methyl styrene dimer ( $\alpha$ -MSD)] as the chain-transfer agent, as shown in Figure 2(d). The mechanism shown was postulated by Meijs and co-workers.<sup>21–23</sup> The structural similarity between  $\alpha$ -MSD

and the terminal double bonds produced by the  $\beta$ -scission reaction makes it likely that this reaction is also important in this polymerization. Woo and Broadbelt<sup>13</sup> and Kruse et al.<sup>19</sup> reported the presence of this reaction in the degradation of polystyrene.

As mentioned previously, in the thermal polymerization of styrene, thermal initiation, polymerization, and polymer degradation occur simultaneously, and the reaction mechanism becomes more complex. The available information, however, is more scarce. Hui and Hamielec<sup>24</sup> and Husain and Hamielec<sup>25</sup> investigated this system up to 200 and 230°C, respectively, and confirmed the initiation and polymerization kinetics; however, a molecular weight description was not achievable by their simplified models. Subsequently, Hamielec et al.<sup>26</sup> investigated the polymerization of styrene and styrene/acrylic acid copolymers in a continuously stirred tank reactor (CSTR) up to 300°C. As with earlier works, it was not possible to adequately describe the average molecular weights or their distributions, although degradation reactions were indicated as the cause of the poor model description. Spychaj and Hamielec<sup>27</sup> investigated the polymerization of styrene/acrylic acid copolymers up to 300°C and concluded that random chain scission and unzipping were important for this polymerization system.

In this work, we consider polystyrene produced by thermal polymerization between 260 and 343°C in a CSTR. This polymer is characterized in terms of its molecular weight distribution (MWD), including significant amounts of specific oligomers, and its chain-end group distribution with various analytical techniques. Because these chain characteristics are determined by the interaction between the various elementary reactions present in the system, from their analysis we can derive precious information about the kinetic mechanisms that dominate the process. In particular, in this work, we concentrate on three specific aspects. We first use preparative gel permeation chromatography (GPC) combined with <sup>13</sup>C-NMR analysis to isolate and identify the characteristic oligomers present in the polymerization product. This allows us not only to determine the mechanism of the specific scission reaction producing each of such oligomers but also to qualitatively estimate their relative rate. The second investigated aspect refers to the presence of branch points along the chain, which indicates whether the produced chains are linear or branched. All the studies on polystyrene degradation mentioned previously were in fact conducted in the absence of the monomer, and so propagation of the midchain radical could not occur. However, in a polymerizing system in which a monomer is available, this might occur, potentially producing a head-to-tail, trifunctional branch point on the chain. It is also possible that termination by combination occurs at this position,

producing a head-to-head branch point. Both of these reactions would have a significant effect on the molecular weight and the polymer microstructure, and so it is important to clarify the extent to which these reactions occur. This is done through a detailed <sup>13</sup>C-NMR investigation of the final polymer.

The last aspect addressed in this work refers to the terminal vinyl double bonds (TDBs) that are produced by  $\beta$ -scission reactions. Actually, the relative importance of the various scission and termination reactions present in the system determines the number of terminal double bonds present in each chain, and so detailed information regarding the distribution of these end groups offers significant insight into the relative importance of these reactions. Matrix-assisted laser desorption/ionization time-of-flight mass spectrometry (MALDI-TOF MS) is a technique that offers this level of chain microstructure resolution and has been used in this study. MALDI-TOF MS is a relatively new analytical tool for polymer characterization, but it has already found numerous applications in determining details of the polymer structure and end groups<sup>28–30</sup> and of the reaction mechanism, such as the relative amounts of termination by combination and disproportionation in polystyrene.<sup>31</sup>

## EXPERIMENTAL

### CSTR experimentation

Styrene was thermally polymerized in a CSTR, operated in the steady state, at temperatures ranging from 260 to 343°C and for residence times ranging from 5 to 90 min, as discussed in detail elsewhere.<sup>32</sup> The CSTR was particularly well suited for high-temperature polymerization because of the very low viscosity of the reacting mixture. After steady state was reached, accurate kinetic data were obtained because of the uniform temperature and concentration conditions inside the reactor. Table I summarizes the experimental runs and the analysis performed on the polymers produced under the various experimental conditions. One selected sample, produced at 316°C with a 15-min residence time, was fractionated preparatively with high-resolution GPC to isolate both the various oligomers produced in the reactor and the various fractions of the polymer with different chain lengths. The identity of each oligomeric peak collected was established with <sup>13</sup>C-NMR, and this enabled the use of GPC for oligomer quantification in all subsequent experiments. Because the position of each oligomeric peak did not change as a function of the reaction conditions, it was assumed that the chemical identity also remained unchanged.

The <sup>13</sup>C-NMR investigation for determining the branching density was performed on polymers produced at 260 and 316°C with a constant residence time

TABLE I  
Reaction Conditions for the Examined Polymer Samples and Analysis Performed

Experimental run	Temperature (°C)	Residence time (min)	Preparative GPC + <sup>13</sup> C-NMR	<sup>13</sup> C-NMR for branching	MALDI-TOF MS
260C/5RT	260	5		✓	
260C/15RT	260	15		✓	
288C/15RT	288	15			✓
316C/15RT	316	15	✓	✓	✓
343C/15RT	343	15			✓

(15 min) to evaluate the temperature effect. In addition, the polymer produced at the lowest temperature and residence time was considered because under these conditions (260°C and 5-min residence time) the highest concentration of the monomer was present, and so the propagation of midchain radicals and the production of head-to-tail branch points were favored. Finally, MALDI-TOF MS was used to identify the end groups on the polymer chains and, in particular, the distribution of terminal double bonds as a function of the molecular weight. Polymers produced at 343, 316, and 288°C with a 15-min residence time were chosen as representatives of the experimental region of study.

### Analytical methods

#### Preparative GPC

Preparative GPC was used to fractionate the polymer sample into various fractions. Through the subsequent analysis (e.g., by NMR) of each fraction, we could estimate various polymer characteristics as a function of its molecular weight. The molecular weights of the polymers were determined by GPC with a Waters 410 differential refractive-index (RI) detector (Milford, MA). For all polymers with sufficiently low molecular weight (all those made above 260°C), a GPC system, particularly well suited to separate low-molecular-weight polymers and oligomers, was used. This system was a Waters 2690 GPC unit equipped with a Shodex guard column (50 mm long, 6-mm inner diameter) and a Shodex HF-2002 column (exclusion limit = 5000; 200-Å Styragel packing) operated at a volumetric flow rate of 1 cc/min. Eight narrow polystyrene standards between 104 and 10,000 Da (Polymer Laboratories, Ltd., Amherst, MA) were used for calibration. This column set exhibited excellent low-molecular-weight resolution, making precise oligomeric determination possible. However, the relatively low exclusion limit made it impossible to measure the highest molecular weight samples in the study, typically those made at 260°C. In those cases, we used two PL-gel mixed-bed columns, each with 10- $\mu$ m-particle-size polystyrene beads, with a single PL-gel preparative guard column. Fifteen narrow polystyrene standards between 104 and 3,000,000 Da were used for

calibration. As expected, this system exhibited no resolution with respect to the low-molecular-weight oligomers. The MWDs are represented in the following with the differential log MWD described by Shortt.<sup>33</sup>

The selected polymer sample was diluted to approximately 0.15 g/L in tetrahydrofuran (THF) and injected successively for a total of 45 injections. Each injection was collected in 72 successive glass vials by a fractionation collector, which deposited 0.5 min of effluent in each vial. Each vial was weighed before use and reweighed after the THF solvent in the vials was evaporated in a ventilated hood for 48 h under ambient conditions.

#### NMR

The NMR instrument used was a Varian Gemini 300 (Palo Alto, CA), a 300-MHz spectrometer. The <sup>13</sup>C spectra were collected with proton decoupling only during acquisition. The pulse width was 2.9  $\mu$ s, and the prepulse delay was 5.0 s, corresponding to an Ernst longitudinal relaxation time ( $T_1$ ) of 500 s. The  $T_1$  values for the carbons measured in this study were all less than 2 s, so the magnetic relaxation between the pulses was expected to be greater than 99.9%. NMR prediction software<sup>34</sup> by ACD, Inc. (Toronto, Canada) was used to estimate the chemical shifts of the various polymer structural details. The chemical shift of each subject resonance was measured with respect to an internal standard, that is, tetramethylsilane. The NMR solvent used was perdeuterated *para*-dioxane. Before each NMR measurement, the homogeneity of the magnetic field and the uniformity of the detector response were ensured by standard tuning protocols.

#### MALDI-TOF MS

The MALDI-TOF instrument used was a Bruker Reflex II (Faellanden, Switzerland) with an N<sub>2</sub> laser at a wavelength of 337 nm. The instrument was calibrated with the proteins Insulin (I-5520; Sigma, Munich, Germany) and Angiotensin II (A-9525; Sigma) and used  $\alpha$ -cyano-4-hydroxycinnamic acid (14,550-5; Aldrich, Munich, Germany) as a matrix. For all the samples, the instrument was operated with gated delayed extrac-

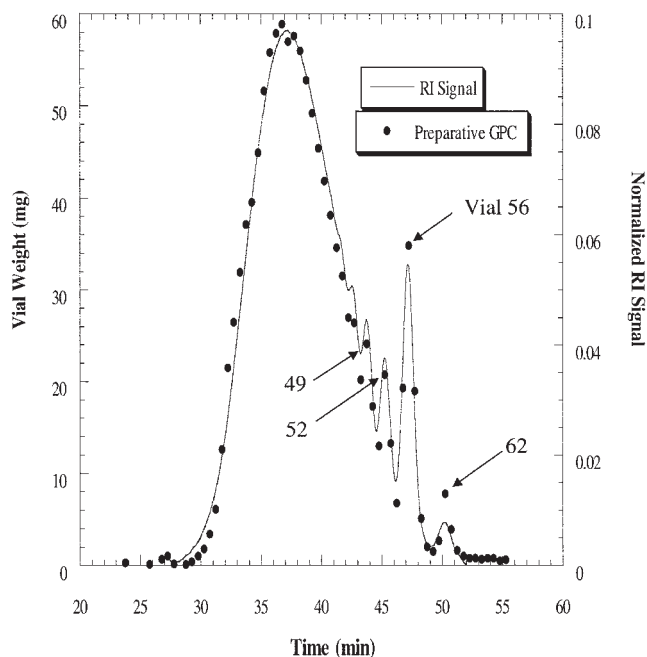


**Figure 3** Weight of the polymer collected in each vial through preparative GPC in comparison with the continuous signal of the RI detector. The numbers indicate the samples (vials) examined in this work.

tion in the positive-ion reflection mode at an accelerating potential of 20 kV, a reflection voltage of 23 kV, and a delay time of 200 ns.

The spectrum for each sample was averaged over 288 laser shots. The matrix and cation used were dithranol and silver, respectively. The polymer samples (0.01M in THF) were mixed with 0.05M (in THF) dithranol and 0.1M silver trifluoroacetate (in THF). The final solution was a 10:10:1 (v/v) polymer/dithranol/silver salt mixture. This matrix/cation combination has been used extensively for polystyrene.<sup>35,36</sup>

## RESULTS AND DISCUSSION

### Oligomer structure identification

The polymer sample used for the identification of the oligomers was produced at 316°C at a residence time of 15 min. The results of the GPC analysis are shown in Figure 3 in terms of the RI detector signal and the weight of the material collected in each vial, measured as described in the Experimental section. The vial number is directly related to the time because each vial contains the material leaving the GPC column for 0.5 min, and so higher vial numbers correspond to lower molecular weights. In Figure 3, distinct peaks appear at the low molecular weights, indicating the presence of the oligomers produced in significant amounts by the back-biting/ $\beta$ -scission reactions mentioned previously. The two low-molecular-weight

peaks that are best resolved are those collected in vials 56 and 62. The structure of each of these samples was analyzed with  $^{13}\text{C}$ -NMR. The polymer peaks corresponding to vials 52 and 49, though resolved to some extent, clearly represented mixtures of oligomers and thus were not analyzed for structure. Instead, the structure of these was inferred from the structure of the two previously identified oligomers and knowledge of the molecular weight from the GPC calibration.

The oligomer collected in vial 62 was identified as DPB, the dimer expected from the 1:3 back-biting/ $\beta$ -scission reaction, as indicated by the comparison of the simulated and experimental  $^{13}\text{C}$ -NMR spectra shown in Figure 4(a,b), respectively. The correct chemical shifts of phenyl head carbons 6 and 12 indicate the presence of the two phenyl units and are corroborated by the two aliphatic carbons 13 and 14. Carbon 16 clearly indicates the terminal unsaturation. There are small, unidentified peaks at approximately 141, 42, and 30 ppm, indicating that the sample was not only pure DPB.

The oligomer collected in vial 56 was identified as TPH, the trimer expected from the 1:5 back-biting/ $\beta$ -scission reaction, as indicated by the comparison of the simulated and experimental spectra shown in Figure 5(a,b), respectively. Particularly convincing is the correct ratio of the phenyl carbons (peaks 11, 17, and 23), confirming the presence of three aromatic rings. Likewise, the presence of the four aliphatic carbons (peaks 1–4) confirms the size of the backbone, providing further evidence of the structure. Finally, peaks 5 and 6, the unsaturated carbons on the terminal double bond, are clearly resolved, confirming the unsaturated nature of this molecule. No cyclic trimer was identified, such as phenyl-4e-(1'-phenyl-ethyl-1')-tetralin, a byproduct of the thermal initiation process, which was reported by other researchers,<sup>6,14,26</sup> and is shown in Figure 1. This trimer was expected to elute at the same elution time as TPH in vial 62 because the two were expected to have similar hydrodynamic volume; however, if it was present, it was below the detection capabilities of the instrument. One possible justification for this finding is that the production of this cyclic trimer is expected to be larger at higher monomer concentrations. Because most of the studies on the thermal initiation process in the literature have been carried out under low-conversion conditions, typically with batch ampule experiments,<sup>11</sup> the monomer concentration was much higher than in the CSTR experiments considered in this work.

The identification of the tetramer (2,4,6,8-tetraphenyl-1-octene) by  $^{13}\text{C}$ -NMR was not attempted because of the partial resolution of the peak associated with vial 52. On the basis of the positive identification of the dimer and trimer, the molecular weight of the peak associated with vial 52 was extrapolated from the GPC

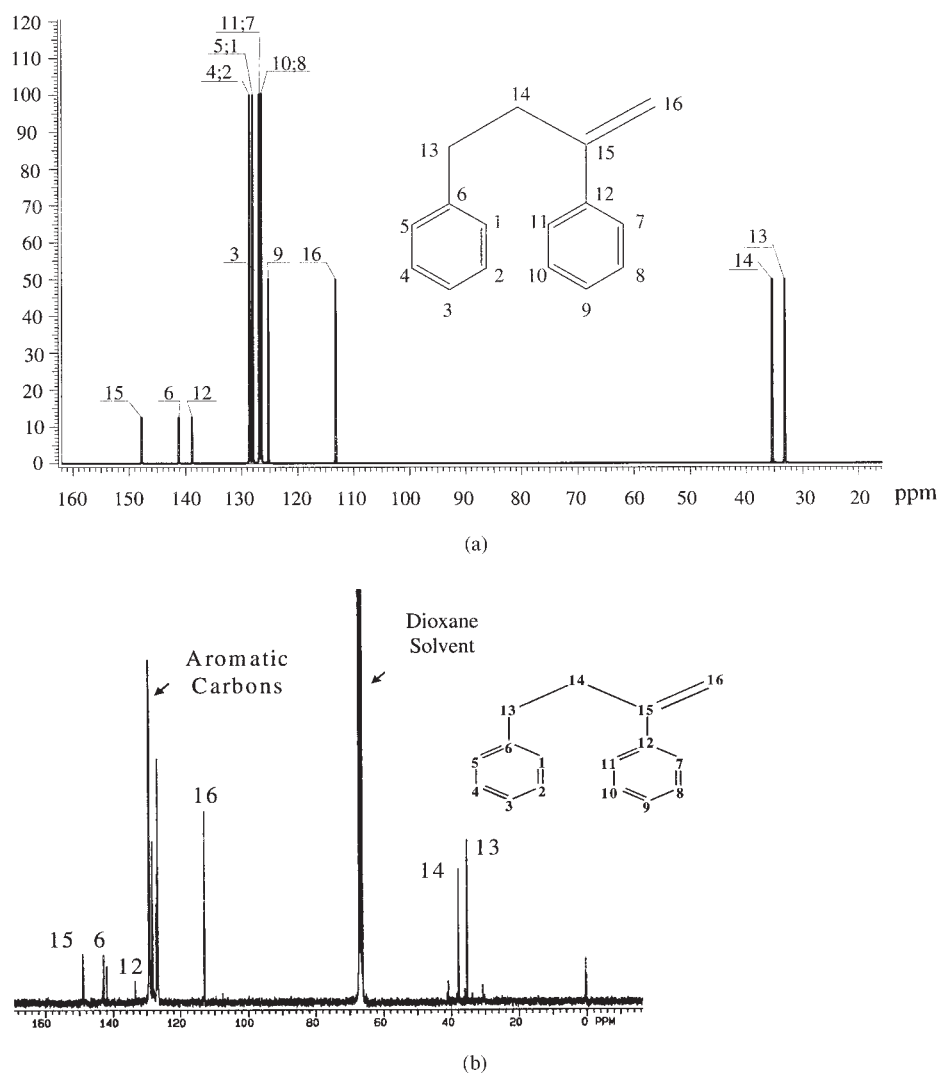


**Figure 4** (a) Predicted  $^{13}\text{C}$ -NMR spectrum for 2,4 diphenyl-1-butene and (b) experimental  $^{13}\text{C}$ -NMR spectrum for the polymer in vial 62.

calibration curve. The molecular weight was estimated to be 412, and so peak 52 was assigned to the tetramer, the product of the 1:7 back-biting/ $\beta$ -scission reaction.

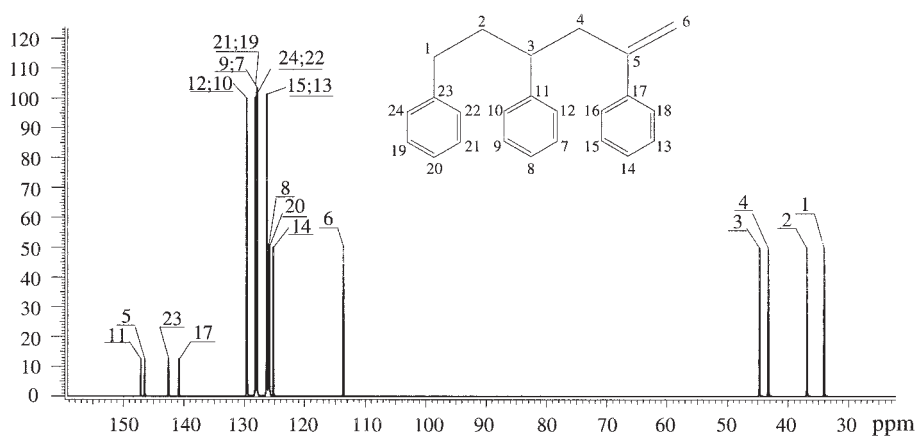
In conclusion, the prevailing dimer, trimer, and tetramer have been identified as DPB, TPH, and 2,4,6,8-tetraphenyl-1-octene in agreement with the findings of Daoust et al.<sup>15</sup> The fact that the trimer is present in much larger proportions than the other two oligomers confirms that 1:5 back-biting is favored with respect to the 1:3 and 1:7 back-biting reactions.

The RI detector was used in a subsequent analysis to quantify the amounts of each oligomer in the distribution through the integration of the weight fraction distribution for the particular fraction of interest. However, the RI signal can deviate from linearity, especially at low molecular weights, and this would render the analysis questionable. To test the validity of integrating the RI signal to quantify the fraction of

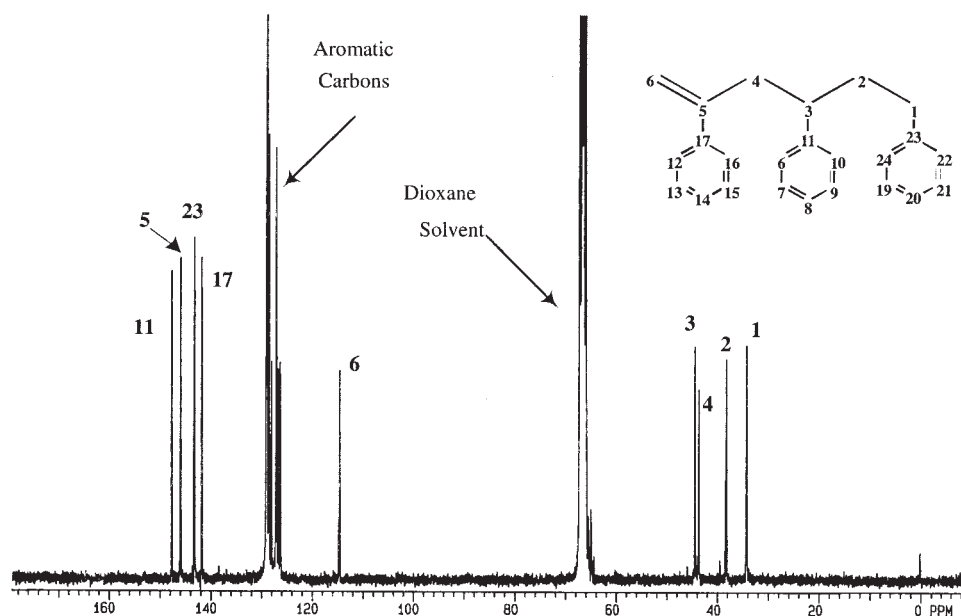
each oligomer in the distribution, we have compared the trimer oligomer fractions calculated from the preparative results with those calculated from the integration of the RI signal. The weight fraction value for the trimer, calculated gravimetrically (preparative GPC), was 6.8%; it was 7.1% from the RI detector. This close agreement confirms the ability to use the RI detector to quantify the low-molecular-weight oligomers.

### Branching

In principle, chain branching occurs if a midchain radical, produced by hydrogen abstraction, either propagates with the monomer or terminates with a growing radical chain. The structure of the branch point is expected to be head-to-tail in the first case and head-to-head in the second. The presence of each of



(a)



(b)

**Figure 5** (a) Predicted  $^{13}\text{C}$ -NMR spectrum for 2,4,6 triphenyl-1-hexene and (b) experimental  $^{13}\text{C}$ -NMR spectrum for the polymer in vial 56.

these structures was investigated through a comparison of computed and experimental  $^{13}\text{C}$ -NMR spectra.

The  $^{13}\text{C}$ -NMR spectrum for a model compound with one head-to-tail branch point was simulated<sup>34</sup> to predict the expected chemical shifts for the branch point and is shown in Figure 6(a). The carbon that identifies this branch point best is the aromatic head carbon adjacent to the branch, designated by carbon number 15. This carbon is expected to be at  $154 \pm 2$  ppm and is sufficiently resolved from the rest of the peaks that it should be clearly distinguishable in the experimental spectrum. The quaternary aliphatic carbon at the branch point (carbon number 23) is expected to be at 34.8 ppm and is not easily distinguishable from the other aliphatic carbons; therefore, it cannot be used. The terminal double bond, designated

by carbon number 51, is also easily seen in the spectrum.

Similarly, a model compound with a head-to-head branch point was simulated and is shown in Figure 6(b). In this case, the modeled spectrum shows that the aromatic head carbon adjacent to the branch point (carbon number 15) is shifted to a lower chemical shift, much closer to the other head carbons, in comparison with the head-to-tail branch point. Therefore, this carbon is not likely to be easily distinguishable in the experimental spectrum. However, the aliphatic carbon adjacent to the branch point (carbon number 52) is shifted sufficiently away from the other aliphatic carbons to be distinguishable, and it was therefore used to identify head-to-head branch points. As in the case of the head-to-tail spectrum, the terminal double bond



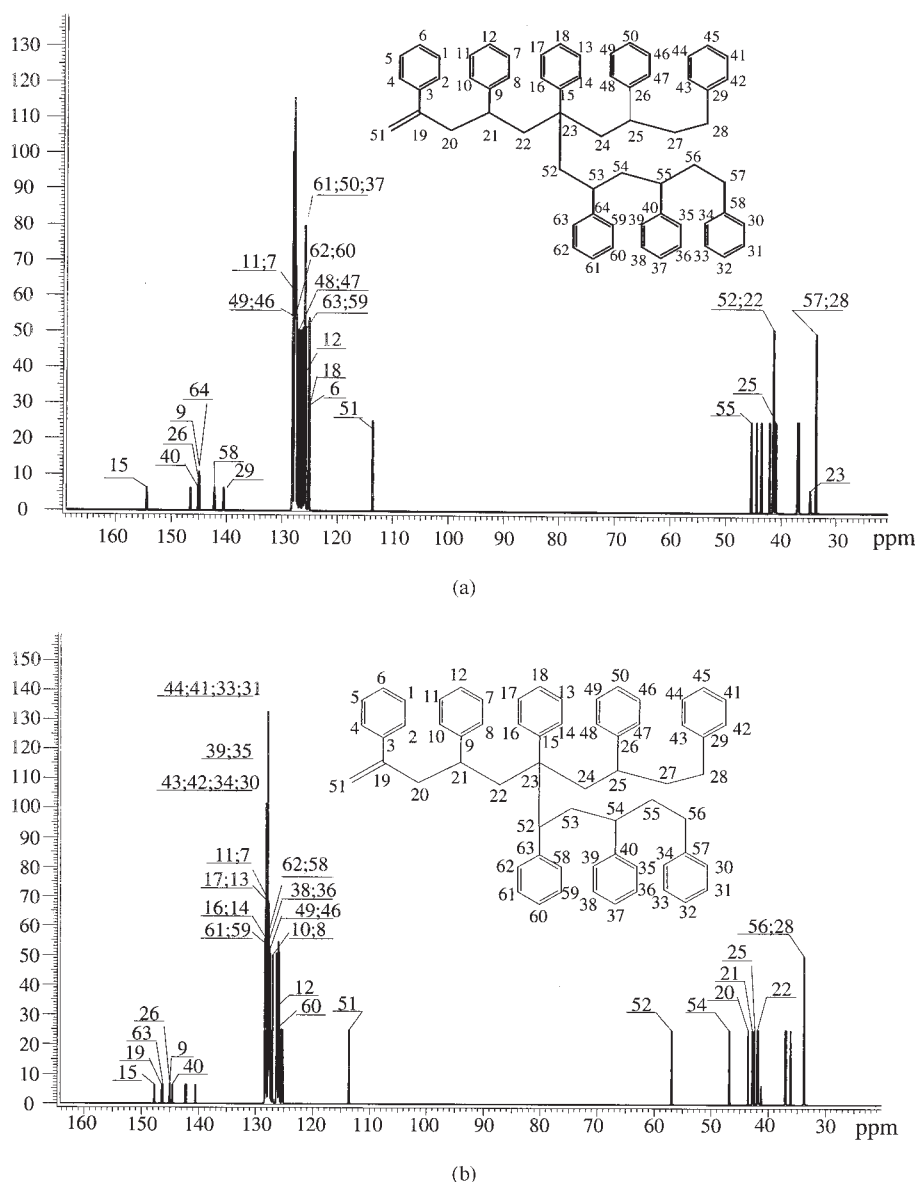


**Figure 6** (a) Predicted  $^{13}\text{C}$ -NMR spectrum of a molecule containing a head-to-tail branch point and (b) predicted  $^{13}\text{C}$ -NMR spectrum of a molecule containing a head-to-head branch point.

is easily distinguished (carbon number 51) at 113.7 ppm. The NMR detection limit for branch points was determined by a signal-to-noise analysis outlined in the appendix.

As shown in Table I, three samples were analyzed for branch points. The first one, corresponding to the experimental run 260C/5RT, was included because it had the highest concentration of the monomer, and so the probability of propagation of the midchain radical was maximum. In the corresponding  $^{13}\text{C}$ -NMR spectra, a representative one of which is shown in Figure 7, none of the characteristic shifts indicated previously for head-to-tail or head-to-head branch points has been found. This means that, if at all present, these branch points have a concentration lower than the signal-to-noise ratio, which

under these conditions means lower than about one branch point per 110 monomer units, as shown in the appendix. Accordingly, from this analysis we can conclude that once midchain radicals are formed by hydrogen abstraction, they do not branch through either propagation or termination to any appreciable extent but exclusively undergo  $\beta$  scission. In addition, it has been proved that under the investigated operating conditions, the thermal polymerization of styrene produces only linear chains.

#### Terminal double-bond distribution

Because all the chains are linear, the only possible end-group combinations in this polymerization are

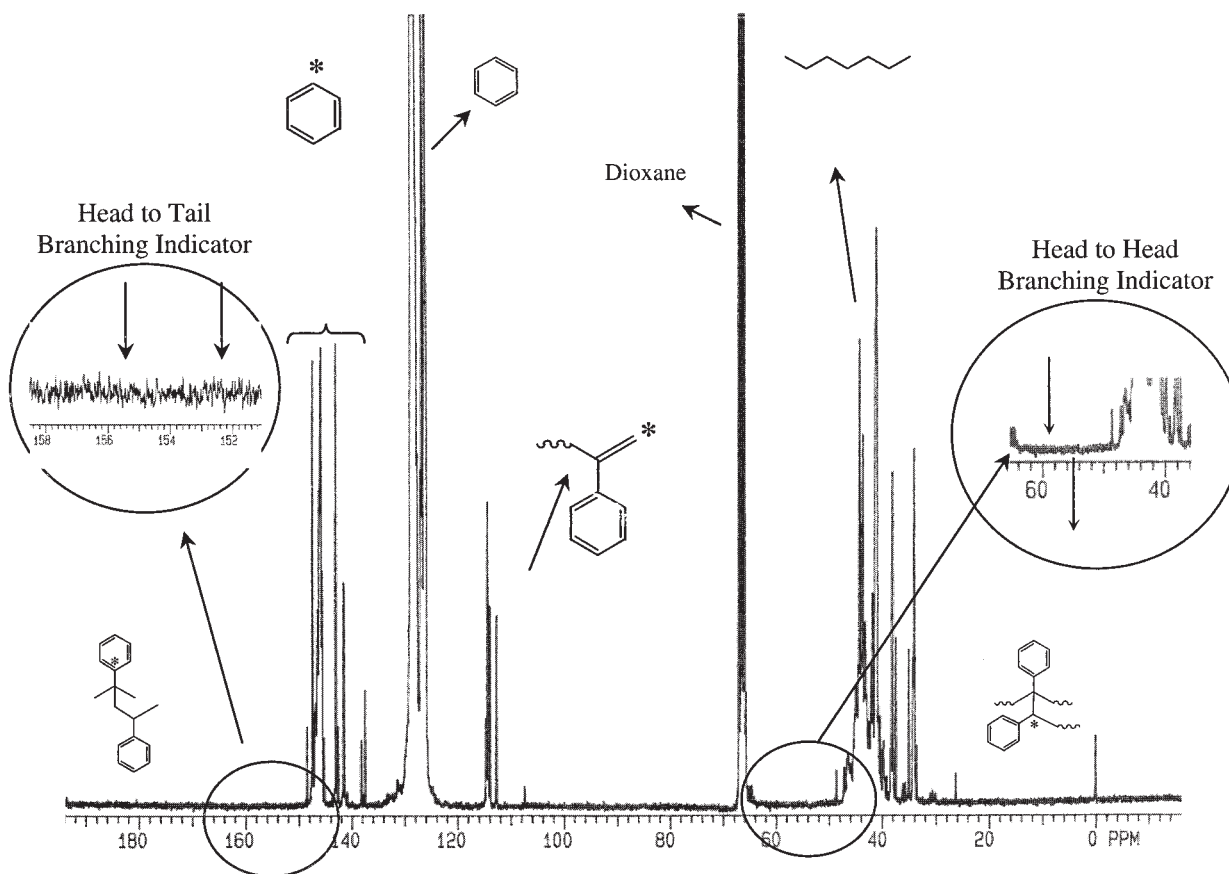


Figure 7  $^{13}\text{C}$ -NMR spectrum of a polymer produced at  $316^\circ\text{C}$  with a 15-min residence time.

chains with zero, one, or two TDBs. Actually, considering the thermal polymerization mechanism of styrene,<sup>5</sup> one could also expect the presence of end groups generated by styrene and 1-phenyl-tetraline radicals produced through a Diels–Alder intermediate (DAI). These are discussed later.

The distribution of TDB end groups is particularly interesting in kinetic studies because it can be directly related to the rates of the reactions responsible for their production. The reaction pathways leading to the various TDB end groups are shown in Figure 8. Polymer chains with zero, one, or two TDBs are represented by  $P_0$ ,  $P_1$ , or  $P_2$ , respectively, and radical chains with zero or one TDB are represented by  $R_0$  or  $R_1$ , respectively. In this reaction schematic, all possible reaction pathways and associated rates consuming and producing each polymer and radical end group are shown. An inspection of these reaction pathways shows that there is no end-group type formed exclusively by a single mechanism. For example, bimolecular termination reactions may produce polymer chains with zero, one, or two TDBs, depending on the specific radicals involved. However, back-biting/ $\beta$  scission always creates a TDB on a polymer chain, so this reaction is never involved in the production of chains with zero TDBs. Chains with zero TDBs are

produced either by the termination of two radicals with zero TDBs or when a radical with zero TDBs abstracts a hydrogen from a polymer chain (CTP). The formation of chains with two TDBs requires the reinitiation of a dead chain with one or two TDBs by CTP. It is not possible to produce chains with two TDBs without a CTP event. On the other hand, back-biting/ $\beta$  scission is a primary route to producing chains with one TDB. Therefore, if the distribution of each of these end groups is known, we can make conclusions regarding the relative importance of bimolecular termination, back-biting, and CTP in the production of polymer chains. The three samples analyzed with MALDI-TOF were produced at 288, 316, and  $343^\circ\text{C}$ , all with a 15-min residence time, to evaluate the impact of temperature on the relative rates of these reactions.

When MALDI-TOF is used for measuring MWDs of polymers, the problem of mass discrimination arises; larger chains can have a lower probability of reaching the detector, and this leads to a misrepresentation of their concentration. This can be due to a variety of factors,<sup>36,37</sup> which in the case under examination here would probably be less severe because of the small range of molecular weights considered. In any case, in this work we have used MALDI-TOF to measure not

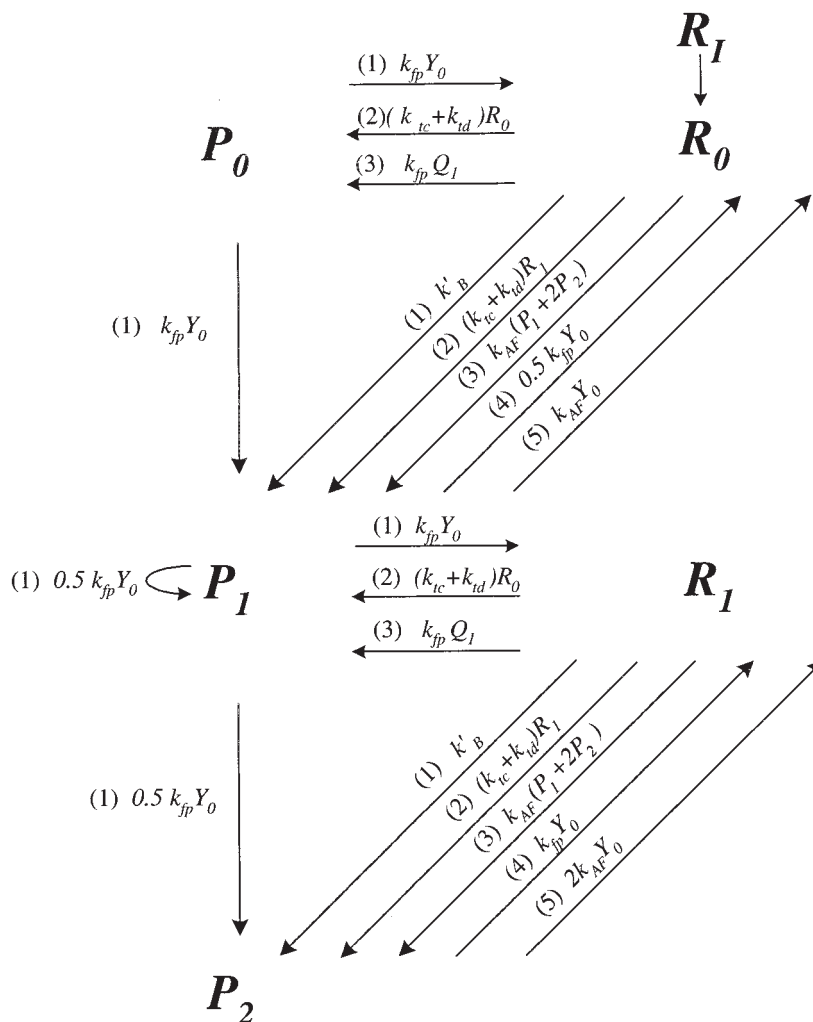
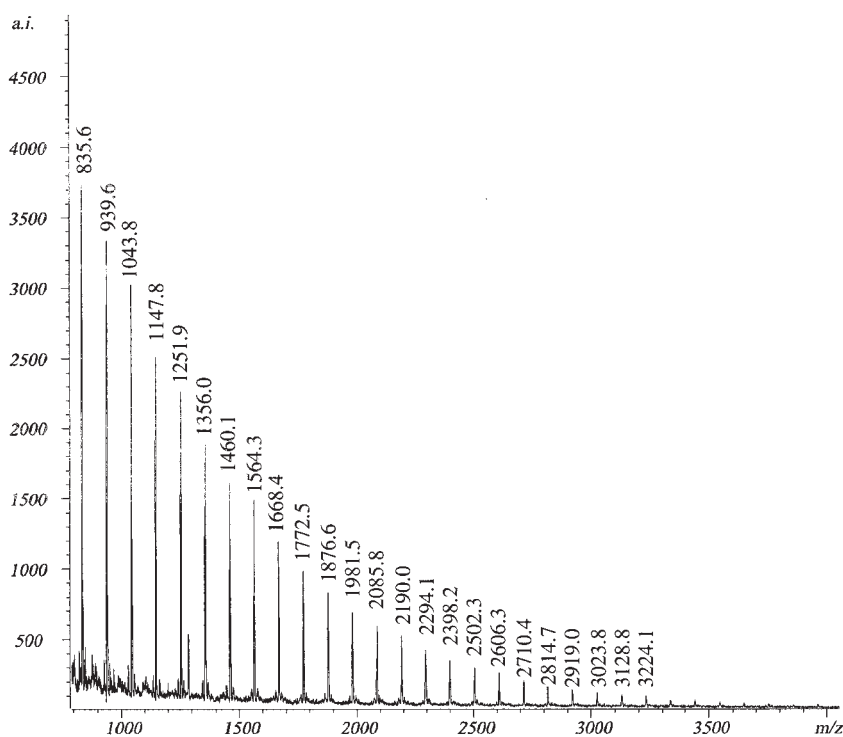


**Figure 8** Mechanistic pathways to chains with zero, one, or two TDBs ( $k_{AF}$  = addition–fragmentation rate constant).

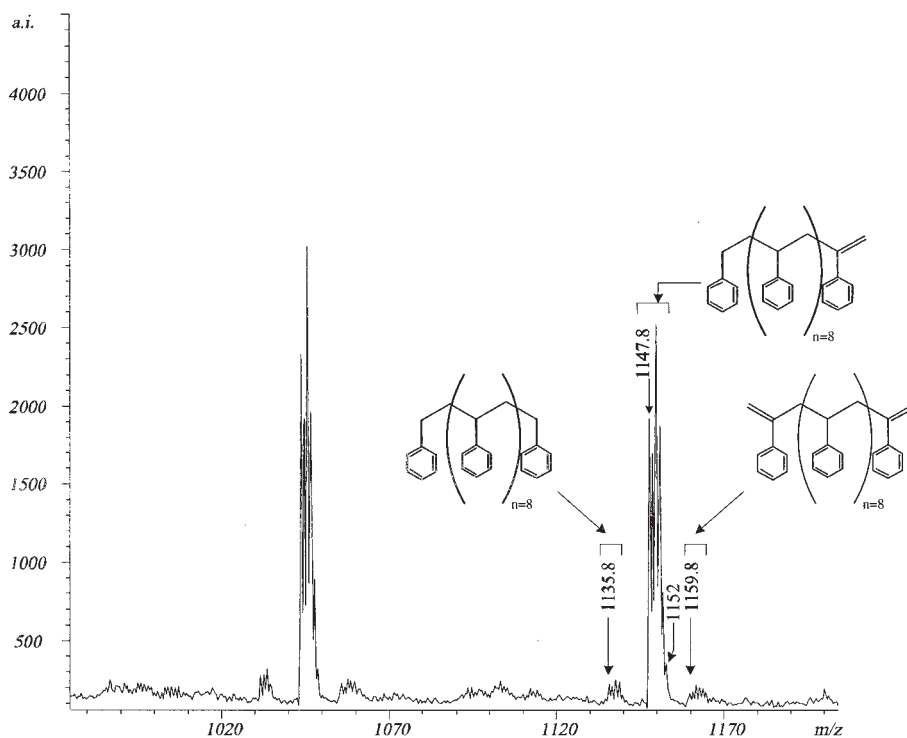
the MWD but rather the relative amounts of chains with different end groups at each chain length. In this respect, it is important that the chains with different end-group moieties are not ionized to different degrees because this would affect the apparent concentration of each particular end group.<sup>38</sup> In this case, the ionizable groups can be assumed to be the double bonds associated with the phenyl groups and the terminal double bonds on the chain. Because the difference in the fraction of the total number of double bonds, and thus the ionizable groups, among chains with zero, one, or two double bonds is small, especially for the longer chains considered in the following, this potential source of error has been ignored.

Figure 9(a) shows the MALDI-TOF spectrum for the sample produced at 316°C. Each pair of successive peaks is 104 Da (equivalent to the molecular weight of one styrene monomer unit) apart, and this indicates that each individual chain length in the distribution has been resolved. Each chain length has been expanded to reveal additional spectral details, and in

particular, chains with mass-to-charge ratios ( $m/z$ ) of 1043.8 and 1147.8, corresponding to chains 9 and 10 monomer units long, are shown in Figure 9(b). Each polymer molecule is associated with a  $Ag^+$  ion, the weight-average molecular weight of which is 107.8 Da. Therefore, the  $[M + Ag^+]$  species that appear in the spectrum at  $m/z = 1043.8$  and  $m/z = 1147.8$  correspond to polymer chains with molecular weight of 936.0 and 1040.0 Da. Each of these main peaks has two additional subpeaks associated with it, appearing at  $m/z = 1135.8$  and  $m/z = 1159.8$ , in the case of a chain length of 10 ( $m/z = 1147.8$ ). The 12-Da difference in these peaks indicates a single carbon atom and implies structures with zero, one, and two terminal double bonds, as shown in Figure 10. Therefore, from the spectra in Figure 9(b), it can be readily concluded that the concentration of chains with one double bond is significantly higher than those with either zero or two double bonds. On the basis of the considerations reported in the context of Figure 8, we can conclude that chain termination is dominated by the back-biting/ $\beta$ -



(a)



(b)

**Figure 9** (a) MALDI-TOF MS spectrum of a polymer produced at 316°C with a 15-min residence time and (b) an expansion of the main peaks at 1045.8–1149.8 Da.

scission reaction. The production of chains with two TDBs must be preceded by CTP, whereas this reaction is not necessarily involved in the production of chains

with one TDB. Therefore, because chains with one TDB dominate, we can conclude that back-biting/ $\beta$  scission is much more important than CTP. This can

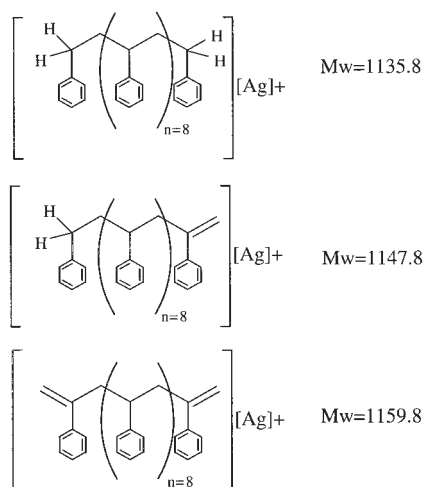


**Figure 10** Molecular structure for polymer chains with 10 monomer units and zero, one, or two TDBs when associated with the silver ion. The corresponding molecular weights can be identified in Figure 9 (b).

be justified by the consideration that although both reactions involve hydrogen abstraction, back-biting/ $\beta$  scission is a unimolecular reaction, with a conformationally favored transition state, whereas CTP is a bimolecular reaction. This conclusion is in good agreement with the results of an independent kinetic analysis,<sup>39</sup> which showed that back-biting/ $\beta$  scission controls the MWD.

The fraction of chains with zero, one, or two TDBs as a function of the chain length was calculated by the integration of each peak in the spectrum in Figure 9(a) and is shown in Figure 11. This fraction does not change significantly as a function of the molecular weight, and this indicates that for these low molecular weights, there is no inhibition of the chain-end mobility due to viscosity, as found by Ide et al.<sup>18</sup> at higher molecular weights. In addition, it might be expected that CTP would be more likely to occur on longer chains, resulting in a higher proportion of chains with two TDBs at higher chain lengths. However, this affect is mild because the chain length dependence on CTP becomes less important at these low chain lengths.

Figure 9(b) also shows that each of the main peaks is subdivided into separate peaks because of the various isotopic combinations possible. There are two isotopes of silver (107.8 and 109.8 Da), each with approximately equal proportions, making each molecular species a doublet. In addition, carbon has two isotopes (12 and 13 Da), with  $^{13}\text{C}$  approximately 1% of the total carbon, and this results in a finite probability that some of the polymer chains will contain  $^{13}\text{C}$  carbon atoms, creating further splitting in the spectrum. Therefore, a chain with a specific number of atoms will have various possible molecular weights because of the isotopes present, producing one distinct peak for each

isotopic combination. The probability of a chain with  $n$  carbon atoms having  $k$   $^{13}\text{C}$  atoms and  $n - k$   $^{12}\text{C}$  atoms is given by

$$P(n,k) = P(\text{C}^{12})^{n-k} \times P(\text{C}^{13})^k \times \left[ \frac{n!}{(n-k)!k!} \right] \quad (1)$$

where  $P(\text{C}^{12}) = 0.989$  is the probability of the occurrence of the  $\text{C}^{12}$  isotope and  $P(\text{C}^{13}) = 0.011$  is the probability of the occurrence of the  $^{13}\text{C}$  isotope (0.011).

Table II shows the molecular structures of the six isotopes expected for a chain containing 10 monomer units with one TDB, together with the molecular weight and molar percentage, which has been computed with eq. (1) and division by two to account for the two silver isotopes. Such relative abundance values are in close agreement with the peak size in the experimental MALDI-TOF spectra shown in Figure 9(b). In particular, from the data in Table II, the molar percentages of 20.8 is predicted for the peak at  $m/z = 1147.8$ , 18.5 is predicted for the peak at  $m/z = 1148.8$ , 29.0 is predicted for the peak  $m/z = 1149.8$ , 20.9 is predicted for the peak at  $m/z = 1150.8$ , 8.2 is predicted for the peak at  $m/z = 1151.8$ , and 2.4 is predicted for the peak at  $m/z = 1152.8$ . These compare quite closely with the areas of the experimental MALDI-TOF peaks, which in the same order lead to 21.0, 18.5, 28.1, 20.6, 8.5, and 3.2%.

Let us now look for the end groups expected from the thermal initiation process. These could be either a methyl end group, originating from a styrene radical, or a 1-phenyl-tetralin end group, originating from a 1-phenyl-tetralin radical. We can inspect the MALDI-TOF spectra for evidence of both of these because they are expected to be comparable in abundance. A

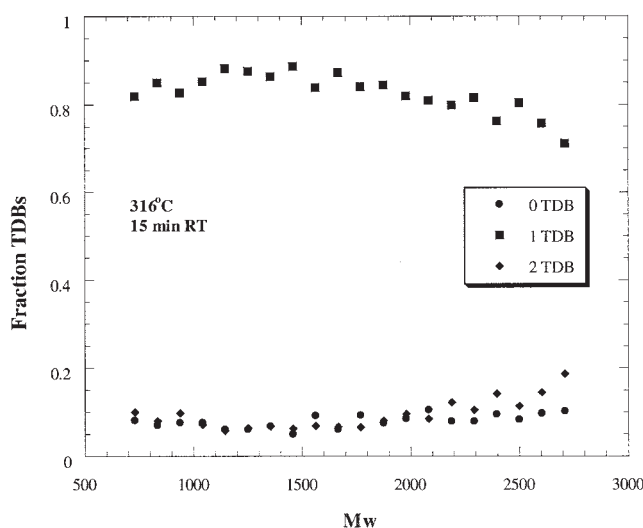
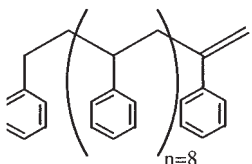


**Figure 11** Fraction of chains with zero, one, or two TDBs as a function of the molecular weight for the spectrum shown in Figure 9 (a).

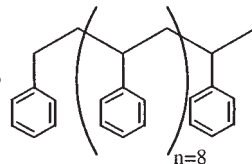
**TABLE II**  
**Isotopic Combinations for a Chain with 10 Monomer**  
**Units with Either 1 TDB or a Methyl End group**  
**Associated with a Ag<sup>+</sup> Ion**

Terminal double bond



Peak	Number of atoms					MW	Abundance (%)
	C <sup>12</sup>	C <sup>13</sup>	H <sup>1</sup>	Ag <sup>107</sup>	Ag <sup>109</sup>		
1	80	0	80	1	0	1147.8	21.1
2	79	1	80	1	0	1148.8	18.7
3	80	0	80	0	1	1149.8	21.1
3	78	2	80	1	0	1149.8	8.0
4	79	1	80	0	1	1150.8	18.7
4	77	3	80	1	0	1150.8	2.2
5	78	2	80	0	1	1151.8	8.0
6	77	3	80	0	1	1152.8	2.2

Terminal methyl group



Peak	Number of atoms					MW	Abundance (%)
	C <sup>12</sup>	C <sup>13</sup>	H <sup>1</sup>	Ag <sup>107</sup>	Ag <sup>109</sup>		
1	81	0	81	1	0	1149.8	21.1
2	80	1	81	1	0	1150.8	18.7
3	81	0	81	0	1	1151.8	21.1
3	79	2	81	1	0	1151.8	8.0
4	80	1	81	0	1	1152.8	18.7
4	78	3	81	1	0	1152.8	2.2
5	79	2	81	0	1	1153.8	8.0
6	78	3	81	0	1	1154.8	2.2

The relative abundance indicates the intensity of the corresponding peak in the MALDI-TOF spectrum. MW = molecular weight.

methyl end group would have a molecular weight 2 Da higher than that of an end group with a TDB. Therefore, the peaks associated with TDBs should have additional peaks associated with them if methyl end groups are significant. Table II reports the isotopes expected from a chain with a methyl end group instead of a TDB. The addition of two protons to the structure with one TDB adds two new peaks at the high-molecular-weight end: one at  $m/z = 1153.8$  and the other at  $m/z = 1154.8$ . An inspection of Figure 9(b) shows no additional peaks at  $m/z = 1153.8$  or  $m/z = 1154.8$ , indicating that if these end groups are present, they must have a very low concentration with respect to the terminal double bond. In addition, the spectra expected for the methyl end group would have a significant peak at  $m/z = 1152.8$ , and this would make this peak significantly higher than that

observed experimentally in Figure 9(b), which confirms that the concentration of this end group is negligible. A similar analysis can be performed for the 1-phenyl-tetralin end group, which is the end group that would be expected for a chain initiated by the DAI. Consider a chain with eight monomer units, terminated at one end with a 1-phenyl-tetralin moiety and at the other with a terminal unsaturation. This chain would exhibit a peak at  $m/z = 1159.8$ , which is clearly present in the spectra in Figure 9(b) but unfortunately overlaps the peak assigned to a chain with two TDBs. On the other hand, we can observe that if the molecular weight development is controlled by chain transfer to the DAI, then we should find chains with two 1-phenyl-tetralin (DAI) end groups and chains with one 1-phenyl-tetralin (DAI) end group and one end group produced by hydrogen abstraction. In the case of chains with eight monomer units, the first ones would produce a peak at  $m/z = 1145.8$ , and the second would produce a peak at  $m/z = 1147.8$ . Actually, only the second is present in the spectrum in Figure 9(b) at the same place that we have assigned to chains with 10 units and one TDB. Finally, the significant peaks seen at  $m/z = 1135.8$  cannot be assigned with this mechanism. These observations are not consistent with a molecular weight development dominated by chain transfer to DAI, whereas they are consistent with our previous conclusion that most chains are formed by back-biting/ $\beta$  scission and not by bimolecular termination or other chain-transfer reactions. In addition, the fact that the concentration of chains with zero and two TDBs is essentially equal can be used to further confirm this conclusion through a kinetic analysis based on the reaction pathways shown in Figure 8 and reported in the appendix.

Figure 12(a) shows the MALDI-TOF spectrum for the sample made at 343°C, the lowest molecular weight sample tested<sup>32</sup> (i.e., number-average molecular weight = 420 and weight-average molecular weight = 570, as measured by GPC). As in the previous example, the main peaks are 104 Da apart (indicating each individual polymerization degree) and are associated with smaller peaks. The oligomer region, at chain lengths of 2, 3, and 4, is particularly interesting. Figure 12(b) shows the individual spectra for the dimer region. As suggested by the <sup>13</sup>C-NMR data, this region should be mainly DPB. When associated with Ag<sup>+</sup>, the  $m/z$  value of this species is 315.8, and the corresponding peaks associated with this set of isotopes can be seen clearly in the spectra. However, the peaks originating from this species and the corresponding isotopes are clearly not the most prominent ones present in this region. The identity of the other peaks is not clear, especially the significant set of peaks associated with isotopes at  $m/z = 331$ . This is approximately 16–17 Da higher than the DPB molec-

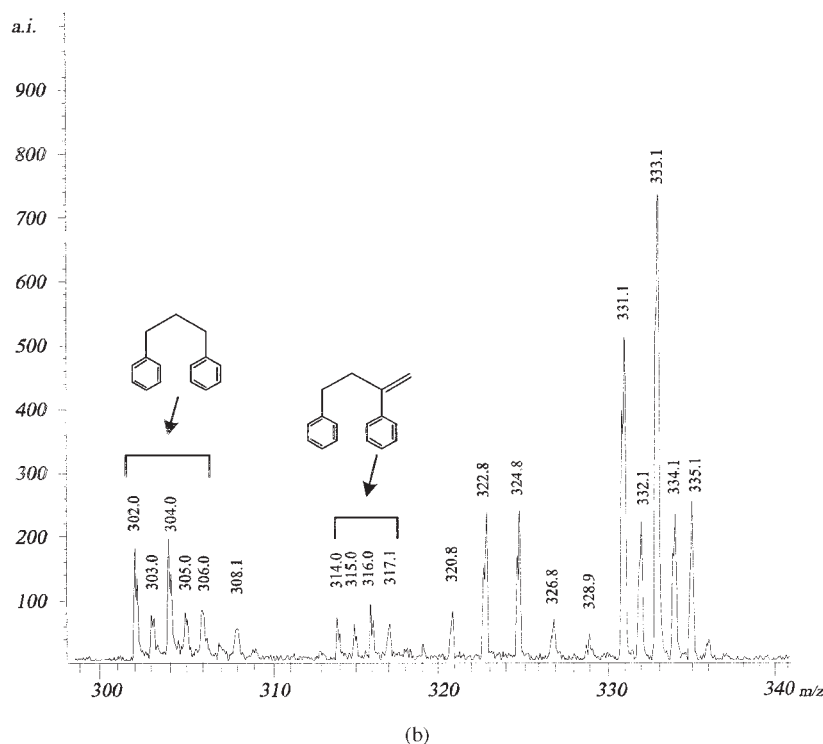
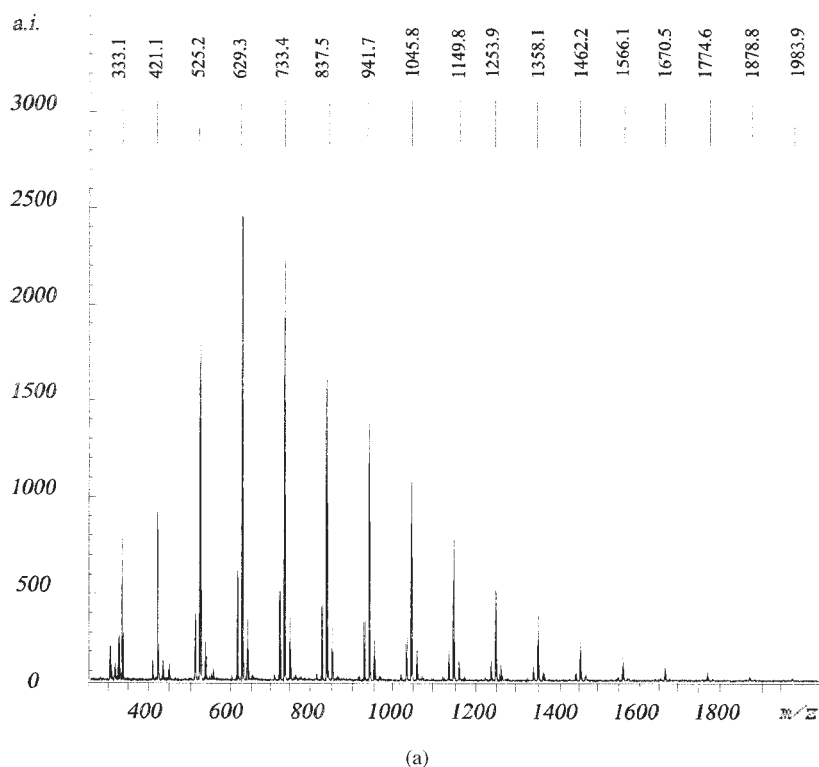
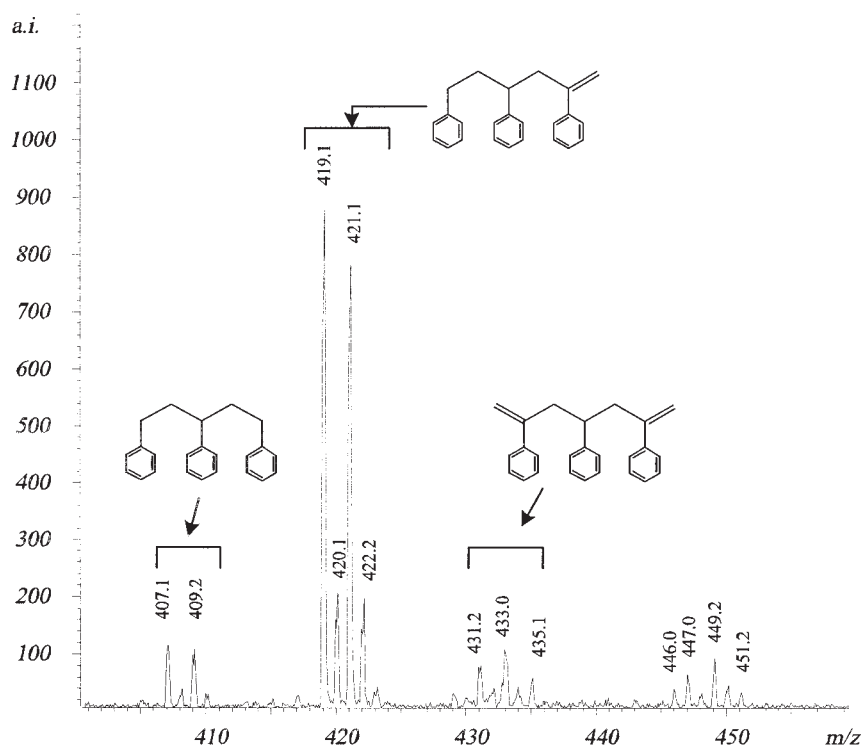


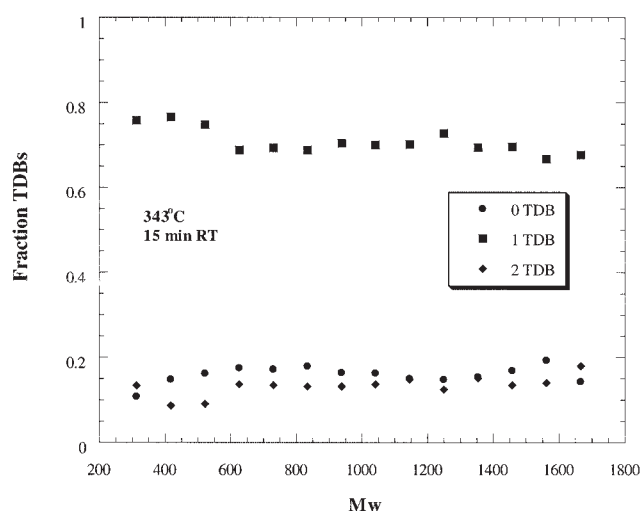
**Figure 12** (a) MALDI-TOF MS spectrum of a polymer produced at 343°C with a 15-min residence time, (b) an expansion of the main peaks in the dimer region, (c) an expansion of the main peaks in the trimer region, and (d) the fraction of chains with zero, one, or two TDBs as a function of the molecular weight.

ular weight but clearly not high enough to be a trimer. These values suggest some type of oxygenated species, possible under these extreme conditions, or interference from the matrix.

Figure 12(c) shows the trimer region, clearly indicating the  $[\text{TPH}][\text{Ag}^+]$  species at  $m/z = 419$ . In addition, the saturated trimer at  $m/z = 407$  and that with unsaturation at both ends at  $m/z = 429$  can be clearly seen.



(c)



(d)

Figure 12 (Continued from the previous page)

Each of the peaks corresponding to the various oligomers, starting from the dimers, has been integrated, and the distribution of the corresponding fractions is shown in Figure 12(d). As at 316°C, the distribution of these end groups remains fairly constant as a function of the molecular weight.

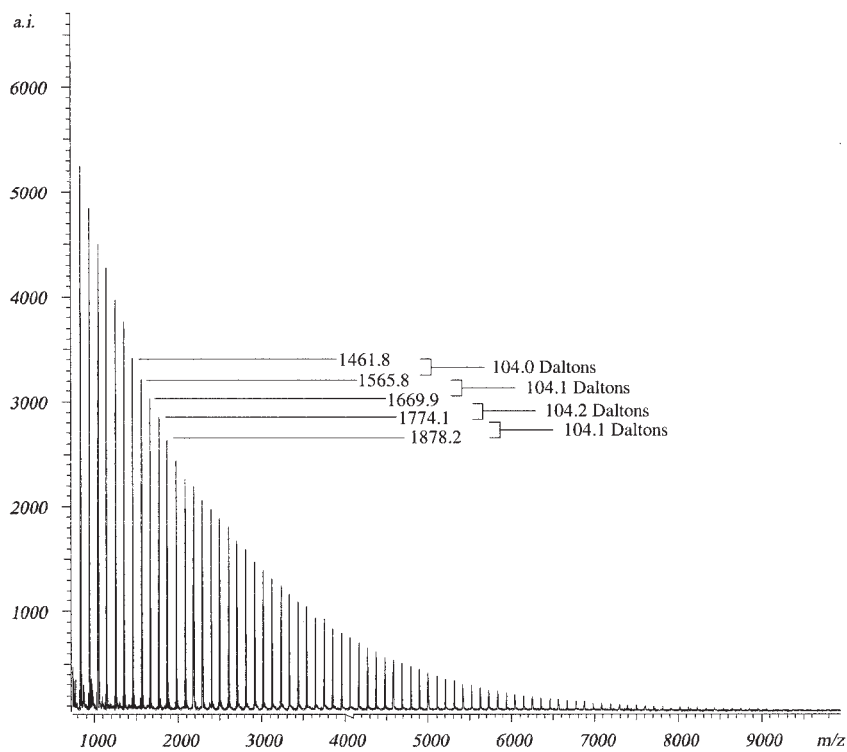
Finally, the MALDI-TOF spectrum from the sample produced at 288°C/15RT is shown in Figure 13(a); a more detailed view of one of the chain lengths is shown in Figure 13(b). This spectrum indicates appar-

ently no major changes in the zero, one, and two TDB distributions as a function of the molecular weight. The corresponding distribution of end groups is shown in Figure 13(c).

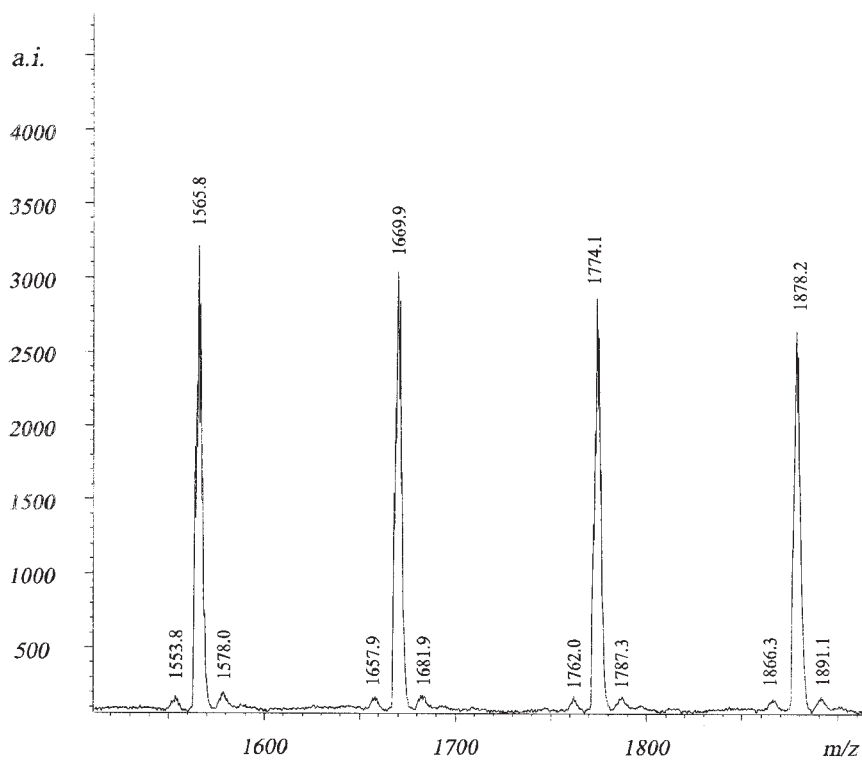
## CONCLUSIONS

The purpose of this study was to elucidate mechanistic details regarding the thermal polymerization of styrene between 260 and 340°C. The data presented here





(a)



(b)

**Figure 13** (a) MALDI-TOF MS spectrum of a polymer produced at 288°C with a 15-min residence time, (b) an expansion of the main peaks at 1500–1900 Da, and (c) the fraction of chains with zero, one, or two TDBs as a function of the molecular weight.

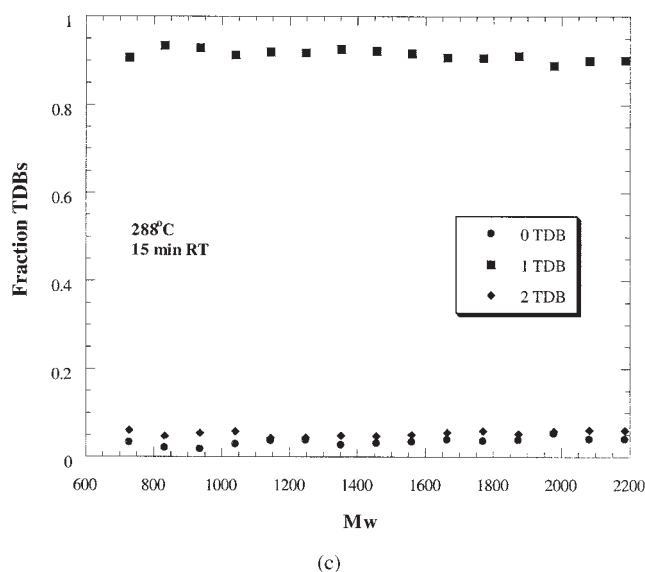


Figure 13 (Continued from the previous page)

indicate a clear mechanistic picture for the polymerization of styrene above 250°C. Back-biting to the third or fifth carbon from the chain end, followed by  $\beta$  scission, is the dominant reaction in the molecular weight development. This conclusion is supported by the  $^{13}\text{C}$ -NMR data coupled with preparative GPC, which showed that the predominant low-molecular-weight oligomers were DPB and TPH, that is, the products of the 1:3 and 1:5 back-biting/ $\beta$ -scission reactions, respectively. The presence of chain-transfer reactions raised the possibility of branching, either from propagation or termination of the midchain radicals. However, head-to-head and head-to-tail branch points were not identified by  $^{13}\text{C}$ -NMR, and this indicated that the midchain radicals underwent  $\beta$  scission before terminating or propagating to any appreciable extent. Finally, the distribution of terminal unsaturations, determined by the relative rates of termination, back-biting, and CTP, was measured with MALDI-TOF mass spectrometry. This showed that the back-biting/ $\beta$ -scission reaction dominated the molecular weight development in comparison with either termination or CTP, thus further supporting our earlier conclusions<sup>32,39</sup> based on an independent kinetic analysis.

The authors thank Dr. Bill Zhu of Johnson Polymer for preparative gel permeation chromatography and nuclear magnetic resonance analysis, Dr. Amrein of ETH (Eidgenössische Technische Hochschule) for the matrix-assisted laser desorption/ionization time-of-flight mass spectra, M. Kaai of Toagosei Co. for very helpful discussions regarding matrix-assisted laser desorption/ionization time-of-flight mass spectrometry, and Johnson Polymer (Racine, WI) for its support of this work.

## APPENDIX

### $^{13}\text{C}$ -NMR detection limits for head-to-tail branch points

In an NMR analysis of polymers, the detector response for the resonance of any given single atom becomes smaller as the polymerization degree increases. Here we want to determine the minimum concentration of head-to-tail branch points in a polystyrene chain that can be detected in an NMR spectrum. This obviously depends on the minimum value of the signal-to-noise ratio ( $S_i/N$ ) that can be detected experimentally, which in our case has been identified as 1.2.

From Beer's law, the intensity of the detector response to an  $i$  component ( $S_i$ ) is proportional to the concentration of that component along the chain ( $C_i$ ), which refers to the number of monomer units in the chain:

$$S_i = kC_i \quad (\text{A.1})$$

To determine the constant  $k$ , we consider the phenyl head carbon 11 on the NMR spectrum for the trimer TPH shown in Figure 5(b), which is chemically similar to the phenyl head carbon associated with the head-to-tail branch point (carbon 15) shown in Figure 6(a). The signal-to-noise ratio ( $S_3/N$ ) for this peak is 43, so using eq. (A.1), we have

$$\frac{S_3}{N} = \frac{k}{N}C_3 = 43 \quad (\text{A.2})$$

Because  $C_3$  is 1/3, we can obtain

$$k = \frac{43N}{C_3} = 129N \quad (\text{A.3})$$

As mentioned previously, the minimum detectable concentration of branch points ( $C_{\min}$ ) is that giving a signal-to-noise ratio equal to 1.2, which means that

$$C_{\min} = 1.2N/k$$

Substituting eq. (A.3) gives  $C_{\min} = 1/108$ ; that is, we cannot detect less than one branch carbon per every 108 units of styrene.

### Kinetic analysis of the MALDI-TOF data

An inspection of the TDB distributions in Figures 11, 12(d), and 13(c) shows that the concentration of chains with zero TDBs is approximately equal to that with two TDBs. This result gives additional insight into the reaction mechanism, and we show that it implies that bimolecular termination is negligible with respect to the sum of back-biting and CTP, thus further supporting our previous conclusion.

The total concentration of chains ( $Q_0$ ) is given by

$$Q_0 = Q_{0,0} + Q_{0,1} + Q_{0,2} \quad (\text{A.4})$$

where  $Q_{0,a}$  is the 0th order moment of polymer chains with  $a$  TDBs, equal to the concentration of chains with  $a$  TDBs.

In the case in which the concentration of chains with zero TDBs equals that with two TDBs, that is,  $Q_{0,0} = Q_{0,2}$ , it follows from eq. (A.4) that the overall concentration of terminal double bonds ( $N_{\text{DB}}$ ) is equal to the overall concentration of chains:

$$N_{\text{DB}} = Q_{0,1} + 2Q_{0,2} = Q_0 \quad (\text{A.5})$$

Because a double bond is formed each time that a  $\beta$ -scission event occurs, and this reaction is always preceded by either CTP or back-biting, the rate of formation of terminal double bonds ( $R_{\text{DB}}$ ) is given by

$$R_{\text{DB}} = k'_B Y_0 + k_{fp} Q_1 Y_0 \quad (\text{A.6})$$

where  $k_{fp}$  is the chain-transfer-to-polymer rate constant,  $k'_B$  is the overall back-biting/ $\beta$ -scission rate constant,  $Y_0$  is the overall 0th moment of the radical distribution (i.e., the total concentration of radicals), and  $Q_1$  is the total concentration of reacted monomer units. The rate of formation of polymer chains ( $R_{pp}$ ) is given by

$$R_{pp} = k'_B Y_0 + k_{fp} Q_1 Y_0 + (k_{tc} + k_{td}) Y_0^2 \quad (\text{A.7})$$

where  $k_{tc}$  and  $k_{td}$  are termination rate constants by combination and disproportionation, respectively. Because eq. (A.2) implies that  $R_{\text{DB}}$  is equal to  $R_{pp}$ , we obtain

$$k'_B Y_0 + k_{fp} Q_1 Y_0 + (k_{tc} + k_{td}) Y_0^2 = k'_B Y_0 + k_{fp} Q_1 Y_0 \quad (\text{A.8})$$

which requires  $(k_{tc} + k_{td}) Y_0^2 \ll k'_B Y_0 + k_{fp} Q_1 Y_0$ . Therefore, we can conclude that the fact that the number of chains with zero and two TDBs is essentially equal implies that bimolecular termination is significantly smaller than the sum of the rates of  $\beta$  scission and CTP. This result is consistent with our earlier conclusion that this polymerization is dominated by the back-biting/ $\beta$ -scission reaction.

## References

1. Mayo, F. R. *J Am Chem Soc* 1968, 90, 1289.
2. Brown, W. G.; Buchholz, K.; Kirchner, K. *Makromol Chem* 1969, 128, 130.
3. Buchholz, K.; Kirchner, K. *Makromol Chem* 1976, 177, 935.
4. Kauffmann, H. F.; Olaj, O. F.; Breitenbach, J. W. *Makromol Chem* 1976, 177, 939.
5. Olaj, O. F.; Kauffmann, H. F.; Breitenbach, J. W. *Makromol Chem* 1977, 178, 2707.
6. Kirchner, K.; Riederle, K. *Angew Makromol Chem* 1983, 111, 1.
7. Jellinek, H. H. G. *J Polym Sci* 1948, 3, 850.
8. Jellinek, H. H. G. *J Polym Sci* 1948, 4, 13.
9. Madorski, S. L. *Thermal Degradation of Organic Polymers; Polymer Reviews 7; Wiley: New York, 1964.*
10. Cameron, G. G.; MacCallum, J. R. *Rev Macromol Chem* 1967, 2, 327.
11. Schroder, U. K. O.; Ebert, K. H.; Hamielec, A. E. *Makromol Chem* 1984, 185, 991.
12. Ebert, K. H.; Ederer, H. J.; Schroder, U. K. O.; Hamielec, A. E. *Makromol Chem* 1982, 183, 1207.
13. Woo, O. S.; Broadbelt, L. J. *Catal Today* 1998, 40, 121.
14. Kurze, J.; Stein, D. J.; Simak, P.; Kaiser, R. *Angew Makromol Chem* 1970, 12, 25.
15. Daoust, D.; Bormann, S.; Legras, R.; Mercier, J. P. *Polym Eng Sci* 1981, 21, 721.
16. McNeill, I. C.; Zulfiqar, M.; Kousar, T. *Polym Degrad Stab* 1990, 28, 131.
17. Ohtani, H.; Yuyama, T.; Tsuge, S.; Plage, B.; Schulten, H. R. *Eur Polym J* 1990, 26, 893.
18. Ide, S.; Ogawa, T.; Kuroki, T.; Ikemura, T. *J Appl Polym Sci* 1984, 29, 2561.
19. Kruse, T. M.; Woo, O. S.; Broadbelt, L. J. *Chem Eng Sci* 2001, 56, 971.
20. Fisher, J. P.; Luders, W. *Makromol Chem* 1972, 155, 239.
21. Meijs, G. F.; Rizzardo, E.; Thang, S. H. *Macromolecules* 1988, 21, 3122.
22. Meijs, G. F.; Rizzardo, E. *Makromol Chem* 1990, 191, 1545.
23. Meijs, G. F.; Morton, T. C.; Rizzardo, E.; Thang, S. H. *Macromolecules* 1991, 24, 3689.
24. Hui, A.; Hamielec, A. E. *J Appl Polym Sci* 1972, 16, 749.
25. Hussain, A.; Hamielec, A. E. *J Appl Polym Sci* 1978, 22, 1207.
26. Hamielec, A. E.; MacGregor, J. F.; Webb, S.; Spychaj, T. In *Polymer Reaction Engineering; Reichert, K. H.; Geisler, W., Eds.; Hüthig & Wepf: New York, 1986; p 185.*
27. Spychaj, T.; Hamielec, A. E. *J Appl Polym Sci* 1991, 42, 2111.
28. Danis, P. O.; Karr, D. E.; Simonsick, W. J.; Wu, D. T. *Macromolecules* 1995, 28, 1229.
29. Shi, S. D. H.; Hendrickson, C. L.; Marshall, A. G.; Simonsick, W. J.; Aaserud, D. J. *Anal Chem* 1998, 70, 3220.
30. Dourges, M. A.; Charleux, B.; Vairon, J. P.; Blais, J. C.; Bolbach, G.; Tabet, J. C. *Macromolecules* 1999, 32, 2495.
31. Zammit, M. D.; Davis, T. P.; Haddleton, D. M.; Suddaby, K. G. *Macromolecules* 1997, 30, 1915.
32. Campbell, J. D.; Teymour, F.; Morbidelli, M. *Macromolecules* 2003, 36, 5491.
33. Shortt, D. W. *J Liq Chromatogr* 1993, 16, 3371.
34. *NMR Prediction Software, version 1.1; ACD (Advanced Chemistry Development): Toronto, Canada, 1995.*
35. Nielen, M. W. F. *Anal Chem* 1998, 70, 1563.
36. Nielen, M. W. F. *Mass Spectrom Rev* 1999, 18, 309.
37. Montaudo, M. S.; Puglisi, C.; Samperi, F.; Montaudo, G. *Macromolecules* 1998, 31, 3839.
38. Rader, H. J.; Schrepp, W. *Acta Polym* 1998, 49, 27.
39. Campbell, J. D.; Teymour, F.; Morbidelli, M. *Macromolecules* 2003, 36, 5502.